

# Rapidly rotating fermions in an anisotropic trap

N. Ghazanfari<sup>1,a</sup> and M.Ö. Oktel<sup>2</sup>

<sup>1</sup> Department of Physics, Middle East Technical University, 06531 Ankara, Turkey

<sup>2</sup> Department of Physics, Bilkent University, 06800 Ankara, Turkey

Received 14 December 2009 / Received in final form 25 May 2010

Published online 2 July 2010 – © EDP Sciences, Società Italiana di Fisica, Springer-Verlag 2010

**Abstract.** We consider a cold gas of non-interacting fermions in a two-dimensional harmonic trap with two different trapping frequencies  $\omega_x \leq \omega_y$ , and discuss the effect of rotation on the density profile. Depending on the rotation frequency  $\Omega$ , and the trap anisotropy  $\omega_y/\omega_x$ , the density profile assumes two qualitatively different shapes. For small anisotropy, the density consists of elliptical plateaus of constant density, corresponding to Landau levels and is well described by a two-dimensional local density approximation. For large anisotropy, the density profile is Gaussian in the strong confining direction and semicircular with prominent Friedel oscillations in the weak direction. In this regime, a one-dimensional local density approximation is well suited to describe the system. The crossover between the two regimes is smooth where the step structure between the Landau level edges turn into Friedel oscillations.

## 1 Introduction

Rotating ultracold gases have received a lot of attention after the initial experimental demonstration of vortices and vortex lattices in a rotating Bose Einstein condensate [1–3]. Beyond vortex physics, these experiments hold promise to create clean, controllable environments to investigate interesting quantum phases brought upon by the unusually high effective magnetic fields created by rotation. There are both theoretical proposals and experimental efforts to investigate vortex lattice melting [4,5], Fractional Quantum Hall states [6–9] and BEC-BCS crossover for rotating gases [10–13].

The usual procedure for rotating gas experiments start by pumping large amount of angular momentum into the cloud by various rotation methods [2,3]. Later, confining the gas into a trap that is as isotropic as possible to preserve angular momentum, the system settles into a ground state that is rotating at some equilibrium frequency. Another alternative route, which is used in at least one experiment [14], is to create a rotating anisotropic trap with some fixed rotation frequency and wait for the system to reach the ground state at this fixed rotation frequency. This procedure allows for one more control parameter, the trap anisotropy, and is theoretically interesting as it allows the system to smoothly go from a two-dimensional regime for small anisotropy to a one-dimensional regime for large anisotropy.

The single particle Hamiltonian for a rotating anisotropic trap is exactly diagonalizable, where the eigenenergies can be found by a Bogoliubov transforma-

tion [15,16]. However, a closed form expression for the real space wavefunctions has not been given until recently [17]. The investigations of rotating anisotropic trap systems have focused either on the properties of vortices, or dynamics in the extremely anisotropic limit [18–20]. All of these studies concern the behavior of interacting Bosons in an anisotropic rotating trap. The interaction strength creates another energy scale which complicates the crossover between the one-dimensional and two-dimensional regimes of the anisotropic trap.

In this study, we consider the density profile for a gas of non-interacting fermions in a rotating anisotropic trap. Because of the Pauli suppression of *s*-wave scattering, spin polarized ultracold fermi gases are naturally non-interacting. The absence of another energy scale related to interactions simplifies the physics considerably and reveals how the anisotropic trap smoothly connects the one-dimensional regime to the two-dimensional regime.

The numerically calculated density profiles clearly show two distinct regimes. For small anisotropy the density profile consists of a ziggurat like structure of elliptical density plateaus. The density inside a plateau is an integer times  $\frac{M\gamma}{2\pi\hbar}$  where  $\gamma$  is a function of trap frequencies and rotation. Each plateau is clearly identified to belong to a Landau level, and this regime can be understood as a small deformation of the quantized density profile in an isotropic rotating trap, which was first discussed by Ho and Ciobanu [21]. As the trap anisotropy is increased, the plateau structure is replaced by a profile that is Gaussian in the strongly confined direction and a sum of semicircles in the weakly confined direction. Friedel oscillations of the density become prominent as this switching happens, and for very large anisotropy the Landau level quantization

<sup>a</sup> e-mail: gnader@newton.physics.metu.edu.tr

is replaced by quantization of the wavefunction along the transverse, i.e. strongly confined, direction. The density profiles give a striking example for smooth connection between the two-dimensional and one-dimensional physics.

The paper is organized as follows: we review the single particle energies and wavefunctions obtained by Fetter for the lowest Landau level [17] in the next section and give the expressions for the wavefunctions in higher Landau levels. In Section 3, we show that the crossover from two to one dimension is already evident in the energy spectra and define the two regimes quantitatively. Section 4 focuses on the numerical density profiles and the description of the properties in both regimes. We also investigate the density profile analytically, and discuss one-dimensional and two-dimensional local density approximation methods along with Friedel oscillations. We conclude in Section 5 by briefly discussing the experimental consequences of our results and indicating directions for future investigations.

## 2 Single particle problem

Our discussion throughout the paper will be limited to behavior in two dimensions. With this limitation, we are able to focus on the physics of switching between one- and two-dimensional regimes without the complications introduced by the motion in the third dimension.

The Hamiltonian for a single particle in a two-dimensional anisotropic harmonic trap can be written in the rotating frame as

$$\mathcal{H} = \frac{1}{2M} (p_x^2 + p_y^2) + \frac{1}{2} M \omega_x^2 x^2 + \frac{1}{2} M \omega_y^2 y^2 - \Omega L_z. \quad (1)$$

Here  $M$  is the mass of the particle, the angular momentum in the  $z$  direction  $L_z$  is given as  $L_z = xp_y - yp_x$ , and  $\Omega$  is the rotation frequency. The trapping frequencies along the  $x$  and  $y$  directions are  $\omega_x$ ,  $\omega_y$ , respectively. Without loss of generality we take  $\omega_y \geq \omega_x$ , and refer to the  $y$  and  $x$  directions as the strongly confined and weakly confined directions throughout the paper.

It is clear from the single particle Hamiltonian that the system is essentially described by two dimensionless parameters, the anisotropy  $\tilde{\omega}_y = \frac{\omega_y}{\omega_x} \geq 1$ , and the scaled rotation frequency  $\tilde{\Omega} = \frac{\Omega}{\omega_x} \leq 1$ .

All the relevant quantities can be non-dimensionalized by scaling all the lengths by the oscillator length in the  $x$  direction  $l_x = \sqrt{\hbar/m\omega_x}$ , frequencies by  $\omega_x$  and energies by  $\hbar\omega_x$ . Our numerical calculations are done in dimensionless units, and we will explicitly state our scaling where appropriate.

The eigenenergies for the Hamiltonian equation (1) can be obtained by a direct diagonalization, or two successive Bogoliubov transformations [15,16]. The eigenstates are labeled by two integers  $n \geq 0$  and  $m \geq 0$ , and the corresponding energy is

$$E_{n,m} = \hbar \left[ (n + \frac{1}{2})\omega_- + (m + \frac{1}{2})\omega_+ \right], \quad (2)$$

where

$$\omega_{\pm}^2 = \omega_{\perp}^2 + \Omega^2 \mp \sqrt{\frac{1}{4} (\omega_y^2 - \omega_x^2)^2 + 4\omega_{\perp}^2 \Omega^2}, \quad (3)$$

with  $\omega_{\perp}^2 = \frac{1}{2} (\omega_x^2 + \omega_y^2)$ .

While the system is controlled by the two dimensionless parameters  $\tilde{\omega}_y$ , and  $\tilde{\Omega}$  a number of other derived parameters give insight into the dynamics and allow one to express results more concisely. The anisotropy of single particle orbits are controlled by two dimensionless parameters

$$\beta_+ = \frac{\omega_x^2 - \omega_{\perp}^2 - \Omega^2}{2\Omega\omega_+}, \quad (4)$$

$$\beta_- = \frac{\omega_{\perp}^2 - \omega_y^2 + \Omega^2}{2\Omega\omega_-},$$

both of which are between 0 and 1. We show in the following sections that a particular combination of these parameters

$$c = \frac{1 - \beta_+ \beta_-}{1 + \beta_+ \beta_-}, \quad (5)$$

controls the switching between the one and two-dimensional regimes. The density of particles in a filled Landau level (see Sect. 4) is related to the frequency

$$\gamma = \frac{\omega_-^2 - \omega_{\perp}^2}{2\Omega}. \quad (6)$$

Finally, we define the two ‘stretched’ complex coordinates which control motion in Landau levels

$$\xi_+ = \sqrt{\frac{2M\gamma\beta_+}{\hbar}} \frac{x + i\beta_- y}{1 + \beta_+ \beta_-}, \quad (7)$$

$$\xi_- = \sqrt{\frac{2M\gamma\beta_-}{\hbar}} \frac{y + i\beta_+ x}{1 + \beta_+ \beta_-}.$$

The ground state of the system has the wavefunction

$$\varphi_{00} = \frac{1}{\sqrt{\pi a_x a_y}} \exp \left[ -\frac{x^2}{2a_x^2} - \frac{y^2}{2a_y^2} \right] \times \exp \left\{ i \frac{Mxy}{\hbar} \left[ \frac{\gamma}{1 + \beta_+ \beta_-} - \frac{1}{2} \left( \frac{\omega_+}{\beta_+} + \frac{\omega_-}{\beta_-} \right) \right] \right\}, \quad (8)$$

where  $a_x$  and  $a_y$  are the widths of the Gaussian envelope

$$a_x^2 = \frac{1 + \beta_+ \beta_-}{\beta_+} \frac{\hbar}{M\gamma}, \quad a_y^2 = \frac{1 + \beta_+ \beta_-}{\beta_-} \frac{\hbar}{M\gamma}. \quad (9)$$

The wavefunctions in the lowest Landau level (LLL) are found by applying the relevant raising operator to be

$$\varphi_{m0}(x, y) = \frac{1}{\sqrt{m!}} \left( \frac{c}{2} \right)^{m/2} H_m \left( \frac{\xi_+}{\sqrt{2c}} \right) \phi_{00}(x, y), \quad (10)$$

where  $H_m$  is the  $m$ th Hermite polynomial.

Another raising operator allows one to generate the wavefunctions in the higher Landau levels, for example

the states in the first excited Landau level have the wavefunction

$$\varphi_{m1}(x, y) = \frac{1}{\sqrt{m!}} \left(\frac{c}{2}\right)^{(m-1)/2} \phi_{00}(x, y) \\ \times \left[ \xi_- \frac{c}{2} H_m \left( \frac{\xi_+}{\sqrt{2c}} \right) - 2im\rho H_{m-1} \left( \frac{\xi_+}{\sqrt{2c}} \right) \right], \quad (11)$$

with  $\rho = \sqrt{\beta_- \beta_+}/(1 + \beta_+ \beta_-)$ . We suggest a general form for wavefunctions in higher Landau levels.

$$\varphi_{mn}(x, y) = \frac{1}{\sqrt{n!m!}} \varphi_{00}(x, y) \sum_{k=0}^n \left[ (-i)^{n-k} \frac{2^{n-k}}{(n-k)!} \rho^{n-k} \right. \\ \times \left. \frac{d^{n-k}}{d^{n-k} \xi_-} P_n(\xi_-) \frac{d^{n-k}}{d^{n-k} \xi_+} P_m(\xi_+) \right] \quad (12)$$

where

$$P_m(\xi_\pm) = \left(\frac{c}{2}\right)^{n/2} H_m \left( \frac{\xi_\pm}{\sqrt{2c}} \right). \quad (13)$$

The wavefunctions given above are remarkable, as they continuously connect the usual 1D harmonic oscillator wavefunctions which have the Hermite polynomial form to 2D Landau level wavefunctions which are (for the lowest Landau level) analytic functions of the complex coordinate  $z = x + iy$ . In the isotropic limit the  $m$ th wavefunction has an  $m$ th order zero at the origin. As the anisotropy is turned on the  $m$ th order zero immediately breaks up into  $m$  first order zeros all of which are on the  $x$  axis, as the roots of Hermite polynomials are always real [16]. Increasing anisotropy separates the roots from each other and forces the Gaussian envelope to be more and more anisotropic.

### 3 One- and two-dimensional regimes

The switching between the two-dimensional and one-dimensional regimes is already apparent in the energy spectrum given in equation (2). It is instructive to consider two limiting cases. The energies of eigenstates of a rotating isotropic trap given as

$$E_{nm} = \hbar \left[ \left( n + \frac{1}{2} \right) (\omega + \Omega) + \left( m + \frac{1}{2} \right) (\omega - \Omega) \right]. \quad (14)$$

The energies for a non-rotating anisotropic trap are

$$E_{n_x n_y} = \hbar \left[ (n_x + \frac{1}{2}) \omega_x + (n_y + \frac{1}{2}) \omega_y \right]. \quad (15)$$

Both of these expressions have the same structure, as they are labeled by two non-negative integers. The rotating anisotropic trap system interpolates between these two limits, and a good identifier for this interpolation is the number of lowest Landau level states that have lower energy than any state in the higher Landau levels. Thus, we define

$$l = \frac{\omega_-}{\omega_+}. \quad (16)$$

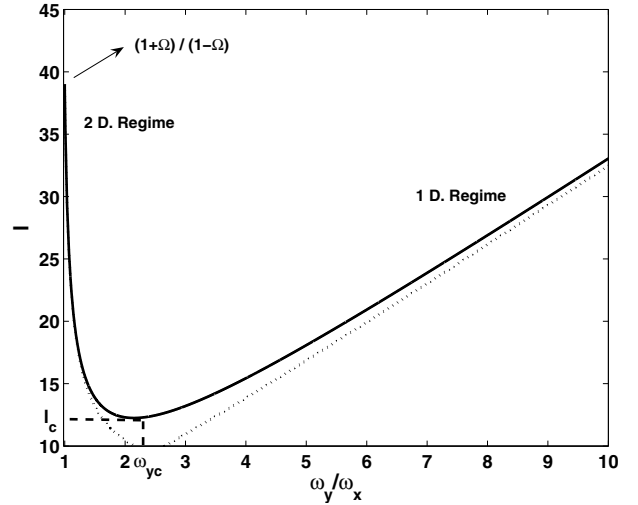


**Fig. 1.** Solid line shows the behavior of  $l$ , number of the stats within two LL's as a function of the anisotropy of the system  $\omega_y/\omega_x$ . Dashed lines are the asymptotic results for one- and two-dimensional limits. Here  $\omega_{yc} = (1 + 4\Omega^2/\omega_x^2)^{1/2}$  is the critical anisotropy where  $l$  is minimum. The minimum number of states is given by  $l_c = (\frac{8}{1-\Omega^2/\omega_x^2})^{1/2}$ . Here  $\Omega/\omega_x = 0.95$ .

The behavior of  $l$  as a function of  $\omega_y/\omega_x$  at rotation frequency  $\Omega/\omega_x$  clearly shows the two regimes (see Fig. 1). At zero anisotropy,  $l$  has its isotropic value  $(1 + \tilde{\Omega})/(1 - \tilde{\Omega})$ . When the anisotropy is introduced, this value quickly decreases as  $\sqrt{\frac{\tilde{\omega}_y^2 - \tilde{\Omega}^2}{1 - \tilde{\Omega}^2}}$  and obtains its minimum value of  $l_{\min} = \sqrt{8/(1 - \tilde{\Omega}^2)}$  at  $\tilde{\omega}_y = \sqrt{1 + 4\tilde{\Omega}^2}$ . As the anisotropy is increased further,  $l$  increases linearly with  $\tilde{\omega}_y$  with slope  $1/\sqrt{1 - \tilde{\Omega}^2}$ . This linear increase is exactly what is expected in the one-dimensional regime as here  $l$  would be the ratio of the effective frequencies in the  $y$  and  $x$  directions,

$$l = \sqrt{\frac{\omega_y^2 - \Omega^2}{\omega_x^2 - \Omega^2}} \simeq \frac{\tilde{\omega}_y}{\sqrt{1 - \tilde{\Omega}^2}}. \quad (17)$$

The degeneracy of the Landau levels in the two regimes originate from two different physical effects. When the anisotropy is small, and the system is in the two-dimensional regime, Coriolis force induced by the rotation partially freezes the kinetic energy of the particles and causes the high degeneracy within the Landau levels. For high anisotropy one can think of the energy spectrum in terms of subband quantization in a narrow channel, where each 'Landau Level' actually is formed by states that have the same wavefunction in the tightly confined direction.

### 4 Density profiles

We now consider the density of a gas of  $N$  non-interacting spinless fermions in a rotating anisotropic trap. As the real space wavefunctions are known the calculation of density reduces to a sum over the absolute squares of the

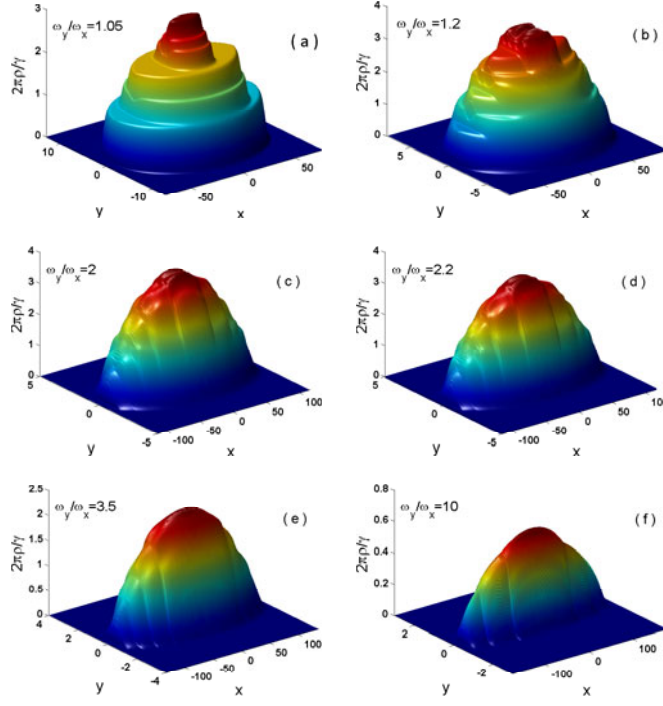


**Fig. 2.** (Color online) Density profiles for fermions at different anisotropy values of the system and fixed number of the particles  $N = 1000$ , and fixed rotation frequency  $\Omega/\omega_x = 0.999$ . The Friedel oscillations are observed in density profiles of anisotropic cases. The number of LL's that fermions fill at each anisotropy can also be determined by counting the number of plateaus in the density profiles.

wavefunctions of all filled eigenstates. Hence the density is given by

$$\rho(x, y) = \sum_{nm} |\phi_{nm}(x, y)|^2 \theta(\mu - E_{nm}), \quad (18)$$

where  $\mu$  is the chemical potential and the energies  $E_{nm}$  and corresponding wavefunctions  $\phi_{nm}$  are given in the previous sections. The chemical potential determined by the number of particles  $N$  in the system with the constraint

$$\int dx dy \rho(x, y) = N. \quad (19)$$

In Figure 2, we display the density profiles for  $N = 1000$  particles with fixed rotation frequency  $\Omega/\omega_x = 0.999$ , for different values of anisotropy. For small anisotropy the density profile mainly consists of steps, with small regions of switching between them. Each plateau is clearly linked with a Landau level, and defines an elliptical area of almost constant density. As shown below, the density contribution from a filled Landau level is  $\rho = \frac{M\gamma}{2\pi\hbar}$ . Thus, the steps have density equal to an integer times  $\frac{\gamma}{2\pi\omega_x}$ . For the parameters in Figure 2a only the lowest three Landau levels have particles and corresponding steps can be identified clearly. The switching between the  $n$ th step and  $(n-1)$ th steps happens with  $n-1$  oscillations in density, which can also be seen in the figure. As the anisotropy

is increased the density oscillations between the Landau level steps become more prominent especially in the weak trapping direction. When the anisotropy is within the critical region of switching between two- and one-dimensional behavior, the steps and the Landau level structure become smeared out. Instead, one can observe the density oscillations becoming prominent throughout the cloud. These oscillations are expected for fermions, as a sharp Fermi surface cutoff in momentum space results in oscillations in real space, known as Friedel oscillations [22] (see Fig. 3). For larger values of anisotropy, the density profile assumes a Gaussian shape in the strong confining direction and the familiar semicircular shape of one-dimensional trapped fermions in the weak confining direction.

To gain a better understanding of the density profile, we investigate the density sum equation (18) in more detail. Let's concentrate on the case for which all the atoms reside in the LLL, for  $N$  particles we can write the sum as

$$\begin{aligned} \rho(x, y) &= \sum_{m=0}^N |\phi_{0m}(x, y)|^2 \\ &= \frac{1}{\pi a_x a_y} e^{-x^2/a_x^2 - y^2/a_y^2} \\ &\times \sum_{m=0}^N \frac{1}{m!} \left(\frac{c}{2}\right)^m H_m\left(\frac{\xi}{\sqrt{2c}}\right) H_m\left(\frac{\xi}{\sqrt{2c}}\right). \end{aligned} \quad (20)$$

In the limit  $N \rightarrow \infty$  this sum can be evaluated using the generating function for Hermite polynomials.

$$e^{-t^2+2tz} = \sum_m \frac{H_m(z)}{m!} t^m, \quad (21)$$

by regarding  $t = |t|e^{i\theta}$  as a complex variable. Then the infinite sum gives the constant density

$$\rho(x, y) = \rho_0 = \frac{1}{\sqrt{1-c^2}} \frac{1}{\pi a_x a_y} = \frac{M\gamma}{2\pi\hbar}. \quad (22)$$

We see that  $\gamma$  is the parameter that controls the density of states per Landau level in an anisotropic trap. In the numerical calculations, we see that the steps in the density profile appear at integer multiples of this value.

The presence of Friedel oscillations in a trapped fermion system is not unexpected, as the physical reason for their presence is the sharp cutoff at Fermi energy. When one is in the two-dimensional Landau level regime the oscillations are suppressed, as locally the maximum allowed density within a Landau level is reached. One can investigate the Friedel oscillations by a simple scaling argument as follows. First let us define the finite sum over Hermite polynomials as

$$S_N(a, b, c) = \sum_{n=0}^N \frac{H_n(\bar{z}) H_n(z)}{2^n n!} c^n, \quad (23)$$

with  $z = a + ib$ . Now because of the infinite sum result we have obtained above we expect two such sums to be

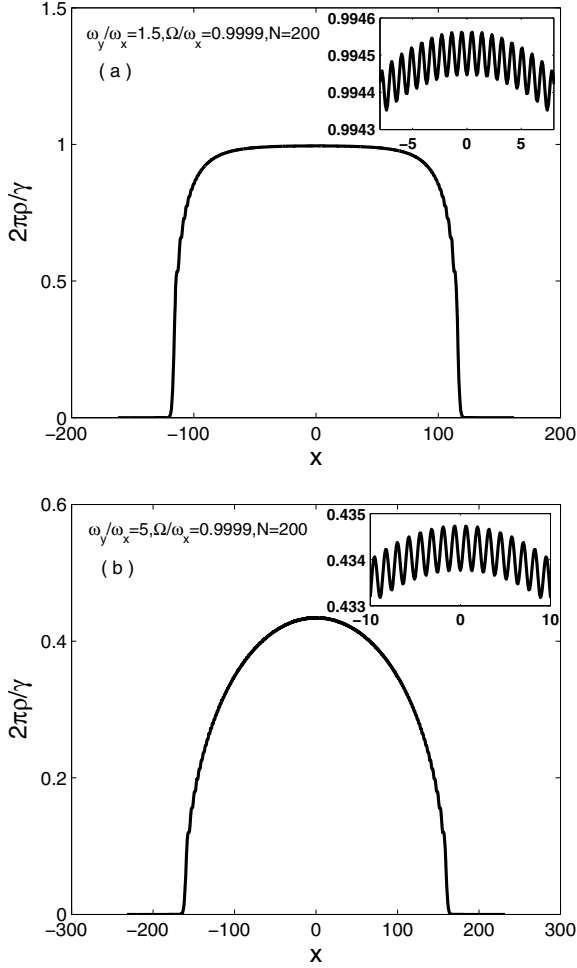


**Fig. 3.** (a) Density for  $N = 200$  fermions at  $\Omega/\omega_x = 0.9999$ , and  $\omega_y/\omega_x = 1.5$ . (b) Density for  $N = 300$  fermions at  $\Omega/\omega_x = 0.999$ , and  $\omega_y/\omega_x = 5$ . The insets in both figures highlight the Friedel oscillation in density profiles of the fermions.

related as

$$S_N(a, b, c_2) \cong \sqrt{\frac{1 - c_1^2}{1 - c_2^2}} \times S_N\left(\sqrt{\frac{(1 + c_1)c_2}{(1 + c_2)c_1}}a, \sqrt{\frac{(1 - c_1)c_2}{(1 - c_2)c_1}}b, c_1\right), \quad (24)$$

if  $N \gg 1$  is sufficiently large. Now  $c_1$  can be chosen arbitrarily close to one, and the resulting sum can be evaluated exactly using Christoffel-Darboux formula [23],

$$S_N(a, b, 1) \approx \sum_{n=0}^N \frac{H_n(\bar{z})H_n(z)}{2^n n!} = \frac{H_{N+1}(\bar{z})H_N(z) - H_{N+1}(z)H_N(\bar{z})}{2^{N+1}N!(\bar{z} - z)}. \quad (25)$$

This exact evaluation and the scaling assumption readily yields a formula for the wavevector of the Friedel oscillations near the center of the trap

$$\rho(x, y = 0) = \rho_0 \left( 1 + (-1)^N \frac{1}{4N} \cos(k_F x) \right), \quad (26)$$

with

$$k_F l_x = \sqrt{8N/\omega_x} \sqrt{\omega_+ + \omega_- \beta_+ \beta_-}. \quad (27)$$

As expected, this scaling result overestimates the amplitude of the Friedel oscillations, especially in the two-dimensional regime. The suppression of oscillations due to limited local density of states is not captured by the scaling assumption. However, scaling correctly describes the wavelength of the oscillations well into the regime where they are too small to observe within our numerical precision.

When the external potential is smooth, a very useful tool to describe the density profile is local density approximation. For the case of a rotating anisotropic lattice we need two different versions of LDA to describe the different behavior in the two regimes.

For the two-dimensional regime the local density at any point of the gas will be an integer multiple of the density of a filled Landau level  $M\Omega/\pi\hbar$ . Thus the density profile within the 2D LDA consists of a sequence of elliptical plateaus, which matches well with the numerically calculated density profiles in the 2D regime. Thus 2D LDA is successful in describing the density profile except for the switching regions between the Landau level steps. A typical plot comparing the result of LDA with the calculated density profile is given in Figure 4.

As the anisotropy is increased and the gas enters the crossover regime the step structure in the density profile is no longer observed. This regime is not well described by a two-dimensional LDA, as the potential in the strong confining direction is no longer smooth on the scale of magnetic length. However, if the anisotropy is increased further, the oscillator length in the strong confining direction becomes much smaller than the magnetic length and another LDA approach becomes feasible. This is exactly the one-dimensional regime described in Section 3.

In the one-dimensional regime, the density profile in the strong confining direction is almost the same for all wavefunctions in the same Landau level. Thus we can treat the system within a one-dimensional LDA and obtain the usual semicircular profile for the one-dimensional fermions

$$\rho(x, y = 0) = \rho(0, 0) \sqrt{1 - \frac{x^2}{L^2}}, \quad (28)$$

where the radius of the cloud is found as

$$L/l_x = \sqrt{\frac{2\mu/\hbar\omega_x - \omega_-/\omega_x}{1 - \tilde{\Omega}^2}}. \quad (29)$$

As can be observed in Figure 4, this approximation describes the density profile in the one-dimensional regime reasonably. The agreement increases with increasing anisotropy, but Friedel oscillations can not be captured within the local density approximation. The agreement of one-dimensional LDA with the numerically calculated

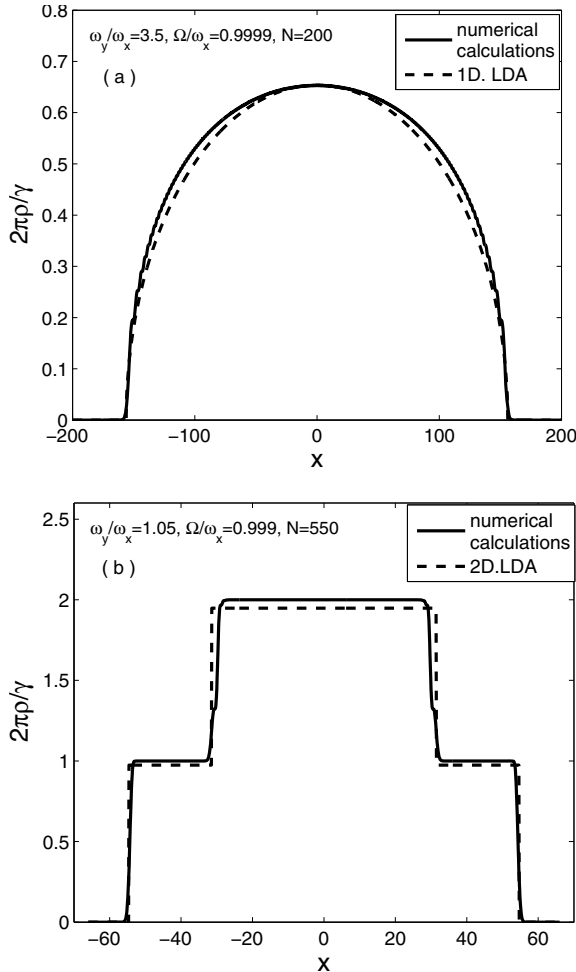


**Fig. 4.** (a) Density of  $N = 200$  fermions obtained by direct numerical calculations (solid line), and one-dimensional LDA (dashed line) at  $\Omega/\omega_x = 0.9999$ , and  $\omega_y/\omega_x = 3.5$ . (b) Density of  $N = 325$  fermions obtained by direct numerical calculations (solid line), and two-dimensional LDA (dashed line) at  $\Omega/\omega_x = 0.99$ , and  $\omega_y/\omega_x = 1.2$ .

profiles further support our interpretation of the very anisotropic Landau levels as sub-bands formed by quantization in the strong confinement direction.

## 5 Conclusion

We show that the density profile of a non-interacting Fermi gas in a rotating anisotropic trap has two distinct regimes depending on the rotation rate and anisotropy. Through numerical calculation and a local density approximation the distinct behavior in the one and two-dimensional regimes is observed. For small anisotropy ( $\omega_y/\omega_x \ll \sqrt{1 + 4\Omega^2/\omega_x^2}$ ), the density consists of elliptical plateaus of constant density, corresponding to Landau levels and is well described by a two-dimensional local density approximation. For large anisotropy ( $\omega_y/\omega_x \gg \sqrt{1 + 4\Omega^2/\omega_x^2}$ ), the density profile is Gaussian in the

strong confining direction and semicircular with prominent Friedel oscillations in the weak direction. In this regime, a one-dimensional local density approximation is well suited to describe the system. The crossover between the two regimes is smooth where the step structure between the Landau level edges turn into Friedel oscillations. Increasing temperature smears out the step structure in the two-dimensional regime, and similarly smoothes out the Friedel oscillation in the one-dimensional regime.

Experiments on rotating ultracold gases have so far focused on isotropic traps. However a rotating anisotropic trap has been demonstrated [14]. A wide array of experiments have displayed the feasibility of designing traps that are strongly confining in one or two dimensions to probe low dimensional physics of quantum gases.

The main method employed in measuring density profiles is expansion imaging of the gas, and this method can be used to determine the main features of the density profile such as Landau level step structure or the semicircular density profile in the one-dimensional regime. More subtle features, such as Friedel oscillations would require more complicated probes of density such as Bragg spectroscopy [24].

Finally, we remark that the Fermi gas in a rotating anisotropic trap is a system that may elucidate the connection between one-dimensional physics with dynamics within a Landau level. It would be interesting to extend the study in this paper to interacting fermion systems.

N.G. is supported by TÜBİTAK. M.Ö.O. is supported by TÜBİTAK-KARIYER Grants No. 104T165 and 109T267.

## References

1. K. W. Madison, F. Chevy, W. Wohlleben, J. Dalibard, Phys. Rev. Lett. **84**, 806 (2000)
2. J. R. Abo-Shaeer, C. Raman, J. M. Vogels, W. Ketterle, Science **292**, 476 (2001)
3. P. C. Haljan, I. Coddington, P. Engels, E. A. Cornell, Phys. Rev. Lett. **87**, 210403 (2001)
4. N.R. Cooper, N.K. Wilkin, J.M.F. Gunn, Phys. Rev. Lett. **87**, 120405 (2001)
5. J. Sinova, C.B. Hanna, A.H. MacDonald, Phys. Rev. Lett. **89**, 030403 (2002)
6. M.A. Baranov, K. Osterloh, M. Lewenstein, Phys. Rev. Lett. **94**, 070404 (2005)
7. A.S. Sorensen, E. Demler, M.D. Lukin, Phys. Rev. Lett. **94**, 086803 (2005)
8. M. Hafezi, A.S. Sorensen, E. Demler, M. D. Lukin, Phys. Rev. A **76**, 023613 (2007)
9. K. Osterloh, N. Barberan, M. Lewenstein, Phys. Rev. Lett. **99**, 160403 (2007)
10. M. Geriner, C. Regal, D. Jin, Nature **426**, 537 (2003)
11. M.W. Zwierlein, C.A. Stan, C.H. Schunck, S.M.F. Raupach, A.J. Kerman, W. Ketterle, Phys. Rev. Lett. **92**, 120403 (2004)

12. M.W. Zwierlein, J. Abo-Shaeer, A. Shirotzek, C.H. Schunck, W. Ketterle, *Nature* **435**, 1047 (2005)
13. I. Bloch, J. Dalibard, W. Zwerger, *Rev. Mod. Phys.* **80**, 885 (2008)
14. P. Rosenbusch, D. S. Petrov, S. Sinha, F. Chevy, V. Bretin, Y. Castin, G. Shlyapnikov, J. Dalibard, *Phys. Rev. Lett.* **88**, 250403 (2002)
15. M. Linn, M. Niemeyer, A.L. Fetter, *Phys. Rev. A* **64**, 023602 (2001)
16. M.O. Oktel, *Phys. Rev. A* **69**, 023618 (2004)
17. A.L. Fetter, *Phys. Rev. A* **75**, 013620 (2007)
18. S. Sinha, G.V. Shlyapnikov, *Phys. Rev. Lett.* **94**, 150401 (2005)
19. P. Sanchez-Lotero, J.J. Palacios, *Phys. Rev. A* **72**, 043613 (2005)
20. A. Aftalion, X. Blanc, N. Lerner, *Phys. Rev. A* **79**, 011603(R) (2009)
21. T.L. Ho, C.V. Ciobanu, *Phys. Rev. Lett.* **85**, 4648-4651 (2000)
22. J. Friedel, *Nuovo Cimento (Suppl.)* **7**, 287 (1958)
23. M. Abramowitz, I. Stegun, *Handbook of Mathematical Functions*, (Dover, New York, 1970)
24. J. Stenger, S. Inouye, A.P. Chikkatur, D.M. Stamper-Kurn, D.E. Pritchard, W. Ketterle, *Phys. Rev. Lett.* **82**, 4569-4573 (1999)